


## ORIGINAL ARTICLE

# Ring1b-dependent epigenetic remodelling is an essential prerequisite for pancreatic carcinogenesis

Simone Benitz,<sup>1,2</sup> Tobias Straub,<sup>3</sup> Ujjwal Mukund Mahajan,<sup>1</sup> Jurik Mutter,<sup>1</sup> Stefan Czernmel,<sup>4</sup> Tatjana Unruh,<sup>5</sup> Britta Wingerath,<sup>5</sup> Sabrina Deubler,<sup>6</sup> Lisa Fahr,<sup>1</sup> Tao Cheng,<sup>6</sup> Sven Nahnsen,<sup>4</sup> Philipp Bruns,<sup>6</sup> Bo Kong,<sup>6</sup> Susanne Raulefs,<sup>6</sup> Güralp O Ceyhan,<sup>6</sup> Julia Mayerle,<sup>1</sup> Katja Steiger,<sup>7</sup> Irene Esposito,<sup>8</sup> Jörg Kleeff,<sup>9</sup> Christoph W Michalski,<sup>9</sup> Ivonne Regel <sup>1</sup>

► Additional material is published online only. To view please visit the journal online (<http://dx.doi.org/10.1136/gutjnl-2018-317208>).

For numbered affiliations see end of article.

## Correspondence to

Dr Ivonne Regel;  
Ivonne.Regel@med.uni-muenchen.de

Received 18 July 2018  
Revised 8 February 2019  
Accepted 24 February 2019  
Published Online First  
6 April 2019



## ABSTRACT

**Background and aims** Besides well-defined genetic alterations, the dedifferentiation of mature acinar cells is an important prerequisite for pancreatic carcinogenesis. Acinar-specific genes controlling cell homeostasis are extensively downregulated during cancer development; however, the underlying mechanisms are poorly understood. Now, we devised a novel in vitro strategy to determine genome-wide dynamics in the epigenetic landscape in pancreatic carcinogenesis.

**Design** With our in vitro carcinogenic sequence, we performed global gene expression analysis and ChIP sequencing for the histone modifications H3K4me3, H3K27me3 and H2AK119ub. Followed by a comprehensive bioinformatic approach, we captured gene clusters with extensive epigenetic and transcriptional remodelling. Relevance of Ring1b-catalysed H2AK119ub in acinar cell reprogramming was studied in an inducible Ring1b knockout mouse model. CRISPR/Cas9-mediated Ring1b ablation as well as drug-induced Ring1b inhibition were functionally characterised in pancreatic cancer cells.

**Results** The epigenome is vigorously modified during pancreatic carcinogenesis, defining cellular identity. Particularly, regulatory acinar cell transcription factors are epigenetically silenced by the Ring1b-catalysed histone modification H2AK119ub in acinar-to-ductal metaplasia and pancreatic cancer cells. Ring1b knockout mice showed greatly impaired acinar cell dedifferentiation and pancreatic tumour formation due to a retained expression of acinar differentiation genes. Depletion or drug-induced inhibition of Ring1b promoted tumour cell reprogramming towards a less aggressive phenotype.

**Conclusions** Our data provide substantial evidence that the epigenetic silencing of acinar cell fate genes is a mandatory event in the development and progression of pancreatic cancer. Targeting the epigenetic repressor Ring1b could offer new therapeutic options.

## INTRODUCTION

Pancreatic ductal adenocarcinoma (PDAC) is a devastating disease with a current 5-year survival rate of 9% and is predicted to be the second leading cause of cancer-related death in the USA by 2030.<sup>1,2</sup> Consequently, the identification of tumour-initiating mechanisms is of great

## Significance of this study

### What is already known on this subject?

- Pancreatic acinar cells show a high cellular plasticity in inflammation-induced regeneration and pancreatic carcinogenesis.
- In acinar-to-ductal metaplasia (ADM) and pancreatic tumour cells, acinar-specific genes are suppressed, whereas embryonic progenitor genes are reactivated.
- Epigenetic modifications largely define gene expression programmes and cellular differentiation.

### What are the new findings?

- The analysis of an in vitro pancreatic carcinogenesis model revealed a broad dynamic epigenetic remodelling of acinar-specific lineage and tumour-associated genes, establishing transcriptional alterations.
- The histone modifier Ring1b catalyses the epigenetic silencing of acinar regulatory transcription factors in ADM and pancreatic cancer cells.
- A conditional depletion of Ring1b prevents ADM and Kras<sup>G12D</sup>-dependent pancreatic tumour formation due to a persistent expression of acinar differentiation genes.
- The epigenetic silencing of acinar cell fate genes is an essential step in pancreatic carcinogenesis, uncovering cellular differentiation as a tumour-suppressive mechanism.

importance to enable early detection and to provide new therapeutic options. PDAC precursor lesions, such as pancreatic intraepithelial neoplasia (PanIN) or atypical flat lesions (AFLs),<sup>3</sup> primarily originate from reprogrammed acinar cells.<sup>4,5</sup> Acinar cells display a remarkable cellular plasticity in pancreatic inflammation (pancreatitis) and transiently transform into a progenitor-like cell type displaying ductal morphology. This process, called acinar-to-ductal metaplasia (ADM), is assumed to facilitate organ recovery after tissue damage.<sup>6</sup> Notably, PDAC development can be triggered through oncogenic



© Author(s) (or their employer(s)) 2019. No commercial re-use. See rights and permissions. Published by BMJ.

**To cite:** Benitz S, Straub T, Mahajan UM, et al. *Gut* 2019;68:2007–2018.

## Significance of this study

## How might it impact on clinical practice in the foreseeable future?

- ▶ The comprehensive epigenetic profiling highlights the dimensions of cellular reprogramming in pancreatic tumour development. By defining epigenetic signatures, benign and malignant cell states might be distinguished, offering a promising strategy for cancer diagnostics.
- ▶ Due to the reversible nature of epigenetic modifications, the restoration of cellular differentiation should be considered as a future therapeutic option. Thus, the epigenetic remodeller Ring1b could be used as a therapeutic target, inducing tumour cell reprogramming in patients with pancreatic ductal adenocarcinoma.

Kras expression in either embryonic acinar or ADM cells.<sup>5,7</sup> In contrast, the expression of mutant Kras<sup>G12V</sup> in fully differentiated, adult acinar cells (AA) rarely induces PDAC.<sup>7</sup> ADM cells are characterised by the establishment of a progenitor-like transcriptional profile due to re-expression of embryonic progenitor genes, such as *Pdx1*, *Rbpj* and *Hes1*,<sup>6,8,9</sup> and downregulation of genes encoding acinar key transcription factors, such as *Ptf1a*, *Rbpjl*, *Bhlha15* and *Nr5a2*, as well as exocrine enzymes, like elastase or amylase.<sup>6,10</sup> Thus, the fundamental changes in gene expression could be an important prerequisite in rendering the cells susceptible to oncogenic cell transformation. However, the molecular mechanisms behind these phenomena are still not fully understood.

In the past decades, driver mutations in *KRAS*, *CDKN2A* (commonly known as p16), *TP53* and *SMAD4* were identified in pancreatic cancer,<sup>11</sup> and global genetic changes were extensively studied within the last years.<sup>12,13</sup> Besides genetic alterations, epigenetic mechanisms were recently found to play a major role in the evolution of metastases of pancreatic cancer<sup>14,15</sup> or in the generation of well and poorly differentiated pancreatic cancer cell types.<sup>16</sup> Methylation, acetylation or ubiquitination of specific lysine residues on histones regulate chromatin compaction, DNA accessibility and gene expression patterns, which define cell identity and differentiation.<sup>17</sup> The methylation of histone H3 on lysine 4 (H3K4me3) promotes active gene expression.<sup>18</sup> In contrast, the monoubiquitination of lysine 119 on histone H2A (H2AK119ub) and the trimethylation of lysine 27 on histone H3 (H3K27me3) act as transcriptional repressors of lineage specific genes or tumour suppressor genes, such as *CDKN2A*, favouring tumour progression.<sup>19</sup> Both modifications are catalysed by the polycomb repressive complexes (PRC) 1 or 2, respectively.<sup>20,21</sup> Until now, the contribution of epigenetic dynamics to acinar cell reprogramming and pancreatic tumour formation has not been specified.

## MATERIAL AND METHODS

## Mice and cell lines

STOCK *Ptf1a*<sup>tm2(cre/ESR1)Cvw/J</sup> (*Ptf1a*<sup>ERT</sup>); B6.129S4-Kras<sup>tm4Tvj/J</sup> (*K\**); B6.Cg-Gt(*ROSA*)26Sor<sup>tm14(CAG-tdTomato)Hze/J</sup> (*tdTomato*) were ordered from The Jackson Laboratory, and *Ring1b*<sup>flox/flox</sup> (*R1b*<sup>f/f</sup>) were kindly provided by Miguel Vidal, Centro de Investigaciones Biológicas-CSIC and Magdalena Götze, Helmholtz Center Munich, Germany. All mice were previously described.<sup>22–25</sup> *Ptf1a*<sup>ERT</sup>-mediated recombination was induced in 6-week-old mice through the administration of 4 mg tamoxifen, bloated in 200 µL of water, by oral gavage on three alternating

days. All mouse experiments and procedures were in accordance with the German Federal Animal Protection Laws and approved by the government of Upper Bavaria for Laboratory Animal Welfare with the reference number 55.2.1.54-2532-119-2015. Pancreatic cancer cell lines were previously isolated from *Ptf1a*<sup>Cre/+</sup>;LSL-Kras<sup>G12D/+</sup> (KC) and *Ptf1a*<sup>Cre/+</sup>;LSL-Kras<sup>G12D/+</sup>;Trp53<sup>lox/+</sup> (KPC) mice. Further information are provided in online supplementary materials and methods section.

All other methods are described in detail in the online supplementary materials and methods section. Primer sequences are listed in online supplementary table 1.

## RESULTS

## Transcriptional changes in pancreatic carcinogenesis are defined by a dynamic epigenetic landscape

To evaluate the sequence of epigenetic reprogramming in PDAC development, we set up an in vitro carcinogenesis model consisting of freshly isolated adult acinar (AA), extracted ADM cells from a three-dimensional (3D) collagen matrix (ADM) and low-passage pancreatic tumour cells (TCs) from a *Ptf1a*<sup>Cre/+</sup>;LSL-Kras<sup>G12D/+</sup> mouse model (figure 1A). Following our isolation procedures, we yielded single cell populations of AA and ADM cells with a purity of more than 90% (online supplementary figure 1A). We further included immature embryonic acinar cells (E18.5) (EA) since ADM and cancer cells exhibit a progenitor-like profile (figure 1A). First, we investigated genome-wide gene expression by conducting mRNA microarray analysis. Hierarchical clustering highlighted a combined cluster of EA, ADM and TC, with EA and ADM showing the closest similarity, whereas AA displayed a distinct gene expression pattern (figure 1B). We detected a good correlation of our AA and TC samples to previously published data sets of murine normal pancreatic tissue and cell lines isolated from tumour specimens (online supplementary figure 1B, online supplementary table 2).<sup>8,26–28</sup>

To uncover gene expression dynamics in EA, AA, ADM and TC, we performed a cluster analysis based on the relative gene expression and identified eight profiles (figure 1C, online supplementary figure 1C and online supplementary table 3). Gene ontology (GO) enrichment analysis was performed for all clusters (online supplementary table 4). Genes in clusters 1 and 4 are associated with the terms 'regulation of Ras protein signal transduction' or 'chromatin modification' (figure 1C and online supplementary table 4). Histone modifiers, such as *Kdm5a* and *Rtf1*, modulating H3K4me3 levels<sup>29,30</sup> or the polycomb group proteins *Ezh2* and *Rnf2* (in the following designated as *Ring1b*), catalysing H3K27me3 and H2AK119ub, respectively, demonstrated an increased expression in EA, ADM and TC, though *Kdm5a* and *Rtf1* expression was absent at the protein level in EA (figure 1C, online supplementary figure 1D and E). These results corroborated our previous findings of an increased *Ring1b* expression in pancreatic carcinogenesis.<sup>31</sup> Moreover, we confirmed the existence of an elevated level of H2AK119ub in EA, ADM and TC, whereas H3K4me3 and H3K27me3 showed an equal distribution among the four biological groups (online supplementary figure 1D,E).<sup>31</sup> Genes in clusters 3 and 8 were upregulated in AA and functionally annotated to the GO terms 'digestion', encompassing acinar digestion enzymes or 'protein transport' (figure 1C and online supplementary table 4). To clarify if these broad transcriptional changes were defined by epigenetic alterations, we performed genome-wide chromatin immunoprecipitation DNA sequencing (ChIP-seq). Here, we globally mapped the transcription activating modification H3K4me3 as well as the PRC-catalysed, repressive histone

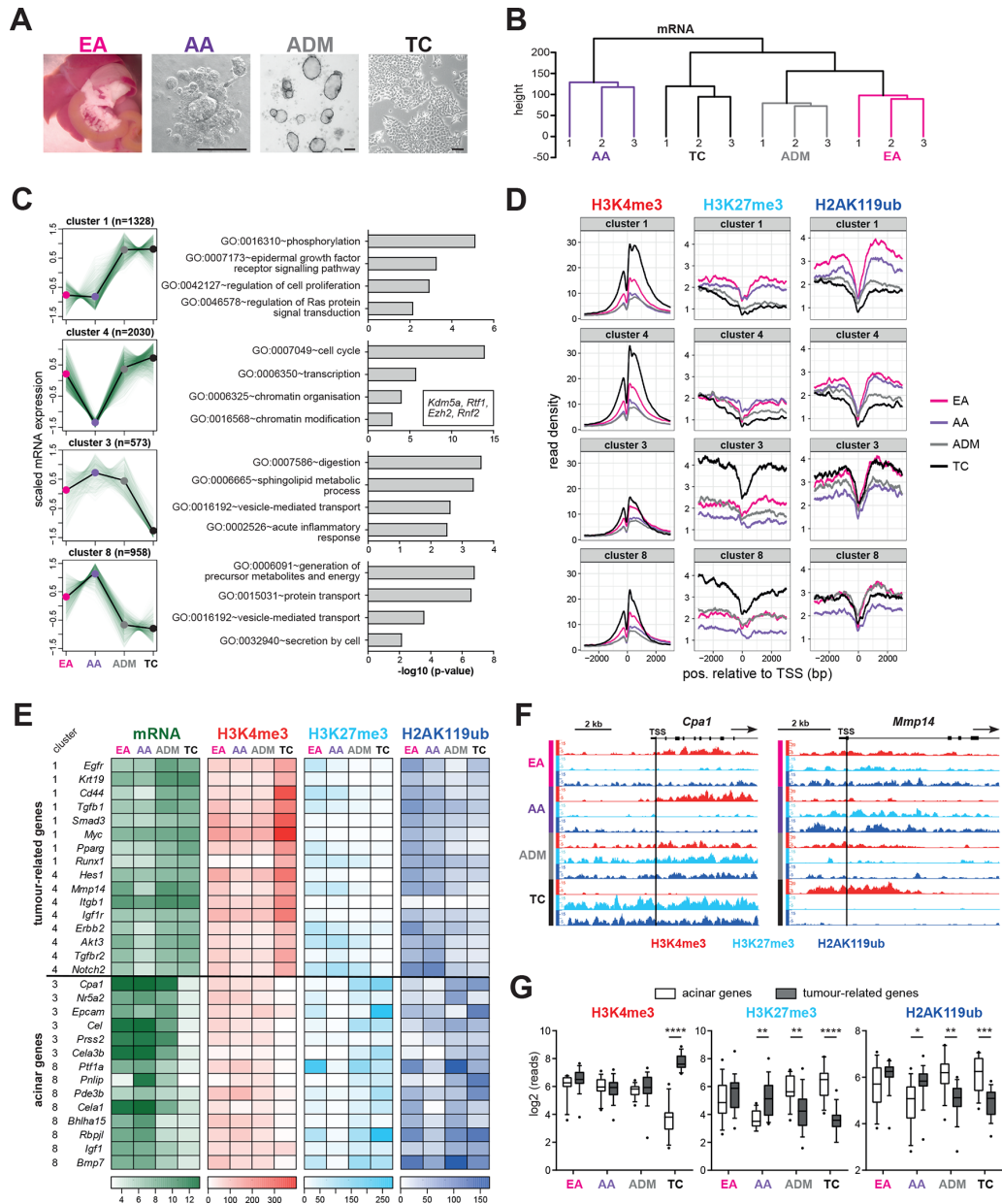


**Figure 1** Transcriptional changes in pancreatic carcinogenesis are defined by a dynamic epigenetic landscape. (A) In vitro carcinogenesis model. Embryonic acinar cells (EA) were isolated from E18.5-staged embryos. Adult acinar cells (AA) were isolated from 8-week-old C57BL/6 mice. AA explants were embedded in collagen to induce acinar-to-ductal metaplasia (ADM) in vitro. Pancreatic tumour cells (TCs) were isolated from a *Ptf1a<sup>Cre/+</sup>;LSL-Kras<sup>G12D/+</sup>* mouse model. Scale bars: 100  $\mu$ m. (B) Hierarchical clustering of microarray samples (each condition, n=3) from the in vitro carcinogenesis model visualised in a dendrogram. (C) Four of the eight clusters determined by k-means clustering of relative gene expression changes were chosen, and related genes were annotated into gene ontology (GO) terms (biological process). A selection of four GO terms with indicated  $-\log_{10}$  p values is shown. (D) Read density plots of ChIP-seq peaks for the three histone modifications H3K4me3, H3K27me3 and H2AK119ub in clusters 1, 3, 4 and 8 around  $\pm 3$  kb of the transcriptional start site (TSS). (E) ChIP signal intensity, measured within 2 kb downstream and 4 kb upstream of the TSS, and relative mRNA expression values from the microarray study are shown in a heatmap for selected acinar and tumour-related genes for each condition. (F) ChIP-seq results at the *Cpa1* and *Mmp14* gene locus. (G) Summarised ChIP signal intensity of H3K4me3, H3K27me3 and H2AK119ub at the selected acinar versus tumour-related genes for each condition. Data are presented as box plots with whiskers indicating the 10th and 90th percentile, respectively; p values were calculated by two-way analysis of variance with multiple comparison; \*p<0.05, \*\*p<0.01, \*\*\*p<0.001, \*\*\*\*p<0.0001.

modifications H3K27me3 and H2AK119ub. H3K4me3 signals were dominantly ( $\sim 80\%$ ) located in promoter regions, whereas H3K27me3 and H2AK119ub were mainly distributed within promoter, intron, enhancer and distal intergenic regions, which is in agreement with previous publications (online supplementary figure 1F).<sup>32 33</sup> For each expression cluster, the distribution

of ChIP-seq signals around the transcriptional start sides is represented as a read density plot (figure 1D and online supplementary figure 1G). Genes from clusters 1 and 4, associated with an increased expression in ADM and TC, showed a strong loss of the repressive H3K27me3 and H2AK119ub in these conditions. In contrast, genes of clusters 3 and 8, related to acinar function,

were characterised by a gain of H3K27me3 and H2AK119ub in EA, ADM and TC (figure 1D). Furthermore, we generated heatmaps, visualising H3K4me3, H3K27me3 and H2AK119ub levels for the genes associated to clusters 1, 3, 4 and 8 (online supplementary figure 2A). We selected previously described acinar or tumour-related genes from each cluster and illustrated the signal intensity of the histone modifications together with the relative mRNA expression levels (figure 1E). Importantly, established acinar differentiation genes, such as *Cpa1*, *Rbpjl* or *Ptf1a*, showed enriched H3K27me3 and H2AK119ub levels along with reduced H3K4me3 and mRNA expression in EA, ADM and TC (figure 1E,F). In contrast, tumour-associated genes, such as *Mmp14* or *Cd44* displayed a strong accumulation of H3K4me3 and a loss of H3K27me3 and H2AK119ub, coinciding with an elevated transcription in TC (figure 1E,F). Altogether, the selected tumour-related genes displayed a significant loss of H3K27me3 and H2AK119ub in ADM and TC. A strong gain of H3K4me3 was solely present in TC. In contrast, known acinar genes were epigenetically silenced by an enrichment of H3K27me3 and H2AK119ub in ADM and TC (figure 1G). Interestingly, a huge loss of H3K4me3 was only observed in TC, suggesting a simultaneous presence of active and repressive histone modifications at acinar genes in ADM.

### Acinar-specific structural and regulatory genes are epigenetically silenced in PDAC development

To uncover further epigenetically regulated target genes in acinar cell reprogramming and pancreatic carcinogenesis, we performed a combined analysis using both our transcriptomic and epigenomic datasets. For the analysis, we selected genes associated with a gain ( $\log_2$  FC >1) or a loss ( $\log_2$  FC <-1) of H3K4me3, H3K27me3 and H2AK119ub within their promoter regions in EA, ADM and TC compared with AA (figure 2A). Notably, the read density of H2AK119ub peaks in promoter and distal regions was the most elevated in EA and ADM, indicating that the enrichment of H2AK119ub in ADM is an important step in acinar cell reprogramming (figure 2B and online supplementary figure 2B). Although H3K27me3 and H2AK119ub showed a broad distribution in distal regions and were highly dynamic in promoter, enhancer and distal regions between EA, AA, ADM and TC (figure 2B, online supplementary figure 1F and 2B), we focused our analysis on promoter regions, since the effect of H3K4me3, H3K27me3 and H2AK119ub on regulating gene expression was previously well defined.<sup>34</sup> Importantly, increased H3K4me3 levels in EA, ADM and TC compared with AA correlated with an upregulated gene expression, whereas the accumulation of the repressive H3K27me3 and H2AK119ub modifications was associated to gene repression (supplementary figure 2C). We performed a gene cluster analysis based on the relative changes in mRNA and histone modification levels and identified eight clusters (A–H), for which we also conducted GO term analysis (figure 2C and online supplementary table 5 and 6). We focused on cluster E (161 genes), since it showed the most dramatic decrease in gene expression together with a loss of H3K4me3 and a gain of H3K27me3 and H2AK119ub in EA, ADM and TC in comparison with AA. This cluster encompassed acinar digestion enzymes, such as *Amy2b*, *Ctrc*, *Prss1* or *Pnlip*, which were functionally assigned to the GO terms ‘proteolysis’ and ‘digestion’ (figure 2D and online supplementary table 6). Moreover, in this group, we detected five transcription factors in total, of which *Ptf1a*, *Rbpjl*, *Bhlha15* and *Nr5a2* were previously described in controlling acinar cell development and homeostasis.<sup>35–38</sup> So far, the Kruppel-like factor 15 (Klf15)

was only described in adipocyte and podocyte differentiation (figure 2D),<sup>39,40</sup> though it may have a role in acinar cell fate determination. As illustrated by figure 2E, the five transcription factors were marked by H3K4me3 in AA, were bivalent in EA and ADM reflected by the simultaneous presence of H3K4me3 and H3K27me3 and/or H2AK119ub and resolved bivalency through a complete loss of H3K4me3 in TC. Dynamic histone patterns correlated appropriately with gene expression (figure 2E). Bivalent chromatin domains are usually established at developmental regulatory genes to maintain an undifferentiated cell identity.<sup>41</sup> Consistently, we detected the highest proportion of bivalent genes in EA and ADM (figure 2F). Of further note, in all conditions, bivalent genes, which exhibited H3K4me3 and H3K27me3 and additionally Ring1b-catalysed H2AK119ub, demonstrated an elevated percentage of regulatory transcription factors (figure 2G). Altogether, by analysing our in vitro carcinogenesis model, we detected a high correlation between changes in gene expression and histone modification dynamics. This study proposes that the accumulation of H3K27me3 and H2AK119ub at acinar differentiation genes in ADM establishes a bivalent status, contributing to the expression of a progenitor-like cell programme, which is also prevalent in EA. A subsequent loss of H3K4me3 during tumour progression strengthens the epigenetic silencing and may manifest TC identity. We confirmed our previous data detecting H2AK119ub accumulation at known acinar cell fate genes<sup>31</sup> and identified novel Ring1b target genes, such as *Klf15*. Based on the prevalence of H2AK119ub at regulatory genes and the increased peak accumulation in ADM, we further aimed to clarify the importance of Ring1b-mediated gene silencing in acinar cell dedifferentiation and pancreatic carcinogenesis.

### Loss of Ring1b impairs pancreatitis-induced ADM

To assess the functional relevance of H2AK119ub gene targeting in acinar cell reprogramming, we generated an inducible *Ptf1a*<sup>Cre<sup>ERT</sup></sup>;Ring1b<sup>flox/flox</sup>;tdTomato<sup>flox/flox</sup> (*Ptf1a*<sup>ERT</sup>;R1b<sup>fl/fl</sup>) mouse model. Depletion of Ring1b in acinar cells was induced at 6 weeks of age, and a recombination rate of ~70% was determined by the tdTomato-reporter expression (online supplementary figure 3A). Under physiological conditions, pancreas histology of adult *Ptf1a*<sup>ERT</sup>;R1b<sup>fl/fl</sup> and *Ptf1a*<sup>ERT</sup> control mice was indistinguishable (online supplementary figure 3B). Inflammation-induced ADM was recapitulated through cerulein injections on two consecutive days. In *Ptf1a*<sup>ERT</sup> control mice, severe ADM formation was detected at days 1 and 2, accompanied by greatly elevated levels of Ring1b and H2AK119ub (figure 3A and online supplementary figure 3C). After 7 days, tissue morphology was restored and Ring1b and H2AK119ub levels descended to normal values (figure 3A and online supplementary figure 3C).<sup>31</sup> Strikingly, *Ptf1a*<sup>ERT</sup>;R1b<sup>fl/fl</sup> mice exhibited significantly fewer ADM and greatly reduced tissue inflammation and fibrosis after cerulein treatment (figure 3A and online supplementary figure 3D). Similarly, 3D acinar cell explants cultured from *Ptf1a*<sup>ERT</sup>;R1b<sup>fl/fl</sup> mice showed reduced ADM formation, validated by a significant reduction in the size and quantity of ADM structures (figure 3B). Immunohistochemical quantification of the acinar marker amylase and clusterin, a marker for cell stress,<sup>42</sup> revealed higher levels of amylase but lower levels of clusterin in cerulein-treated *Ptf1a*<sup>ERT</sup>;R1b<sup>fl/fl</sup> animals (figure 3C). In addition, a lower number of CD45-positive cells was detected in *Ptf1a*<sup>ERT</sup>;R1b<sup>fl/fl</sup> mice (online supplementary figure 3E). Moreover, immunoblot analysis confirmed decreased protein levels of Ring1b and H2AK119ub in cerulein-treated *Ptf1a*<sup>ERT</sup>;R1b<sup>fl/fl</sup>

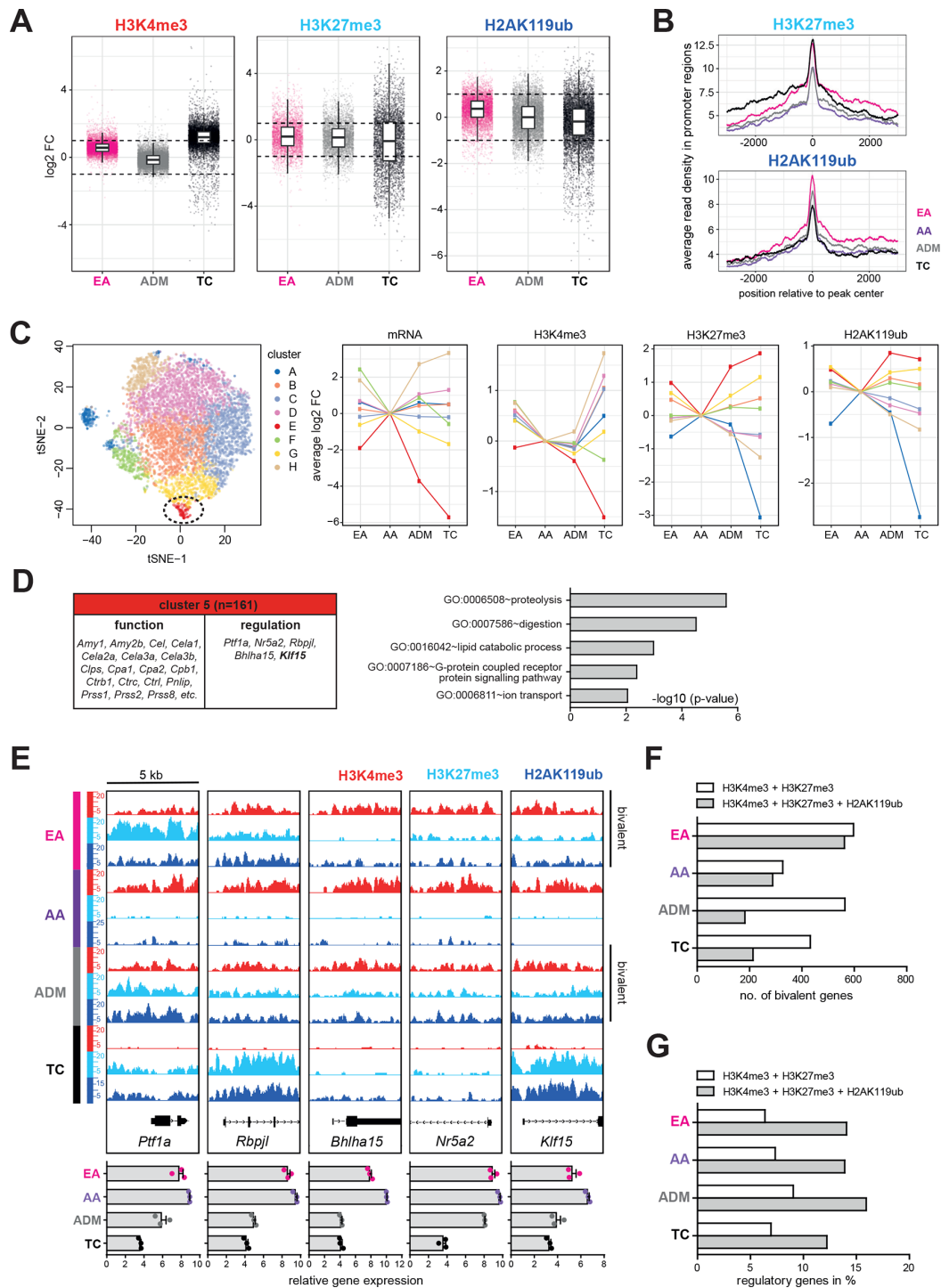


**Figure 2** Acinar-specific structural and regulatory genes are epigenetically silenced in PDAC development. (A) Log<sub>2</sub> fold changes (FCs) of H3K4me<sub>3</sub>, H3K27me<sub>3</sub> and H2AK119ub levels in EA, ADM and TC in comparison with AA. Only 'active genes' exhibiting a substantial number of reads (H3K4me<sub>3</sub>: 64 reads; H3K27me<sub>3</sub> and H2AK119ub: 32 reads) in at least one condition were considered (n=8329, 3847 and 6643 for H3K4me<sub>3</sub>, H3K27me<sub>3</sub> and H2AK119ub, respectively). A log<sub>2</sub> FC >1 was considered as a gain, whereas a log<sub>2</sub> FC <-1 was regarded as a loss of the histone modification. (B) Distribution of the average read density of H3K27me<sub>3</sub> and H2AK119ub ChIP-seq peaks located in promoter regions is plotted ±3 kb around the peak centre for EA, AA, ADM and TC. (C) A total of 9778 'active genes' showing differential mRNA expression as well as ChIP signal changes relative to AA were subjected to k-means clustering and visualised using t-distributed stochastic neighbor embedding (tSNE). Gene expression (mRNA) and histone modification dynamics of the eight clusters are represented. (D) Candidate genes from cluster 5, involved in acinar-specific cell function and regulation, are depicted. The five most significant GO terms are listed, and p values are represented as -log<sub>10</sub>. (E) ChIP-seq reads of the five regulatory transcription factors within a 5 kb frame containing the TSS. The corresponding relative gene expression levels are indicated below. (F) Genes with a simultaneous presence of H3K4me<sub>3</sub> and H3K27me<sub>3</sub> or H3K4me<sub>3</sub>, H3K27me<sub>3</sub> and H2AK119ub in their promoter regions were considered as bivalent. (G) The two groups of bivalent genes were compared with a list of 2329 transcription factors (defined by GO:0006355, GO:0003700 and GO:0043565) to determine the number of regulatory genes. AA, adult acinar cell; ADM, acinar-to-ductal metaplasia; EA, embryonic acinar cell; GO, gene ontology; TC, tumour cell.

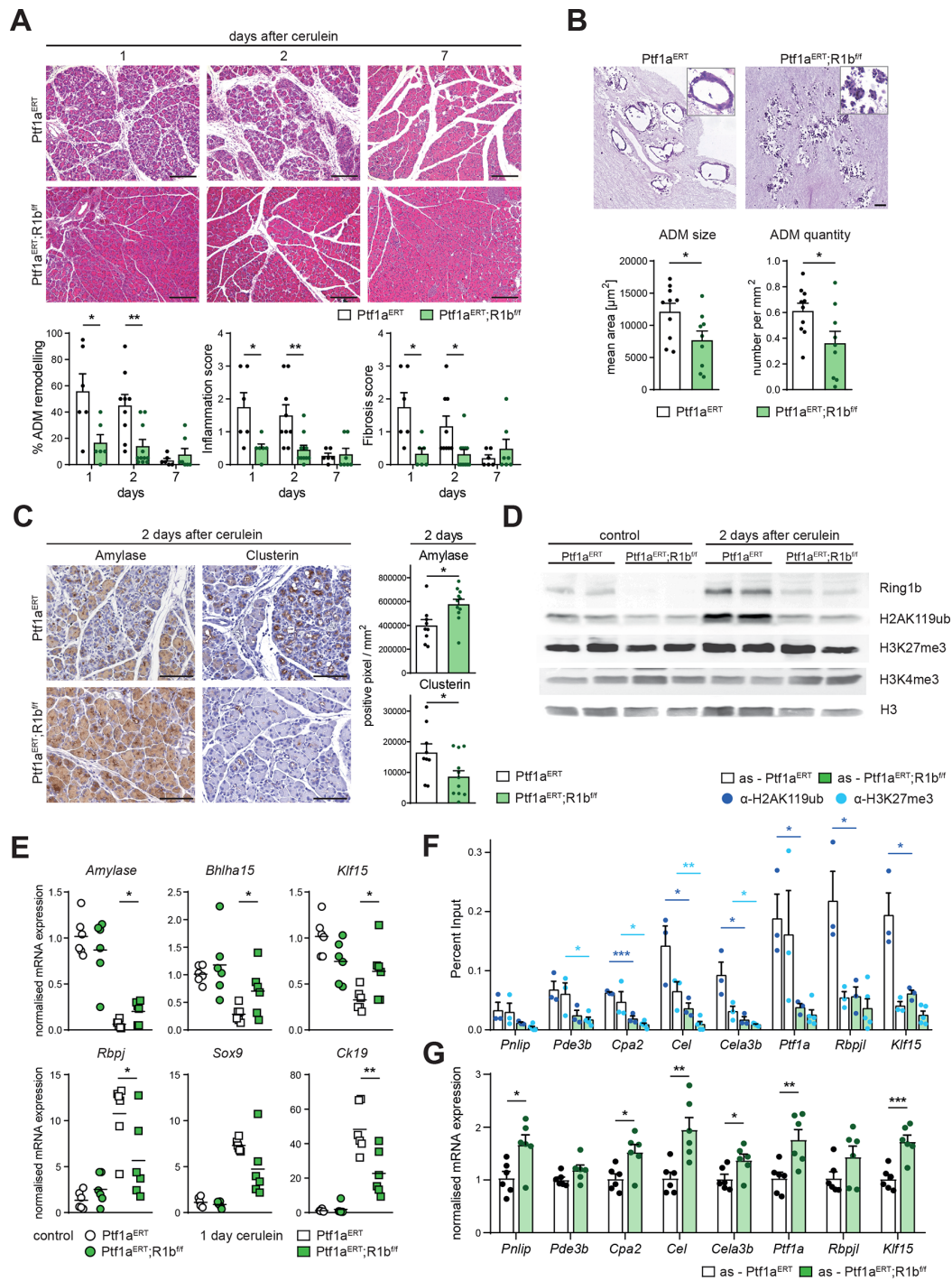


**Figure 3** Loss of Ring1b impairs pancreatitis-induced acinar-to-ductal metaplasia (ADM). (A) Ptf1a<sup>ERT</sup> and Ptf1a<sup>ERT</sup>;R1b<sup>fl/fl</sup> mice were treated with tamoxifen (6-week-old) and cerulein (8-week-old). Representative H&E staining is shown for 1, 2 and 7 days after the last cerulein injection. Scale bars: 200  $\mu$ m. Quantity of ADM remodelling was estimated in per cent to the whole slide. Severity of inflammation and fibrosis was scored. Data are represented as mean $\pm$ SEM; p values for the inflammation and fibrosis score were calculated by Mann-Whitney test (n=6–11). (B) Representative images of three-dimensional acinar cell explant cultures from ten Ptf1a<sup>ERT</sup> and nine Ptf1a<sup>ERT</sup>;R1b<sup>fl/fl</sup> mice. Scale bars: 100  $\mu$ m. Total number of ADM was quantified per mm<sup>2</sup> and ADM size was determined as mean area [ $\mu$ m<sup>2</sup>] by using QuPath. (C) Representative pictures of amylase and clusterin immunohistochemistry from animals sacrificed 2 days after the last cerulein administration. Scale bars: 100  $\mu$ m. Whole tissue staining was quantified with QuPath through positive pixel count (n=9–11). (D) Representative immunoblot analysis of protein lysates from control and cerulein-treated (2-day time point) Ptf1a<sup>ERT</sup> and Ptf1a<sup>ERT</sup>;R1b<sup>fl/fl</sup> mice with the indicated antibodies. Histone H3 served as loading control (n=2). (E) mRNA expression analysis of acinar differentiation and progenitor genes in control and in cerulein-injected Ptf1a<sup>ERT</sup> and Ptf1a<sup>ERT</sup>;R1b<sup>fl/fl</sup> mice (1-day time point) (n=6). (F) ChIP analysis of H2AK119ub and H3K27me3 at the promoter sites of indicated acinar-specific genes of suspension-cultured acinar cells (as) (24 hours) originating from Ptf1a<sup>ERT</sup> and Ptf1a<sup>ERT</sup>;R1b<sup>fl/fl</sup> mice. ChIP DNA was quantified by qRT-PCR and normalised as per cent of input (n=3). (G) mRNA expression of indicated genes in 24 hours suspension-cultured acinar cells (as) from Ptf1a<sup>ERT</sup> and Ptf1a<sup>ERT</sup>;R1b<sup>fl/fl</sup> mice was determined by qRT-PCR (n=6). Unless otherwise stated, all data are represented as mean $\pm$ SEM; p values were calculated by two-tailed, unpaired Student's t-test; \*P<0.05, \*\*p<0.01, \*\*\*p<0.001.

mice, whereas the global amounts of H3K4me3 and H3K27me3 remained unaffected (figure 3D). Notably, 1 hour after the final cerulein injection, we did not observe any significant differences in the pancreas-to-body weight ratio and in serum lipase and LDH levels between Ptf1a<sup>ERT</sup> and Ptf1a<sup>ERT</sup>;R1b<sup>fl/fl</sup> animals, suggesting that the mice were equally challenged (online supplementary figure 3F). However, we detected a significantly higher mRNA expression of the acinar differentiation genes *Amylase* and *Bhlha15*, as well as of *Klf15* in cerulein-treated Ptf1a<sup>ERT</sup>;R1b<sup>fl/fl</sup> mice in comparison with treated Ptf1a<sup>ERT</sup> animals (figure 3E and online supplementary figure 1G). On the contrary, expression of progenitor and ductal genes, such as *Rbpj* and *Ck19*, was markedly reduced in cerulein-treated Ptf1a<sup>ERT</sup>;R1b<sup>fl/fl</sup> animals compared with treated Ptf1a<sup>ERT</sup> mice (figure 3E). In order to prove that acinar differentiation genes are direct targets of Ring1b, we performed ChIP of acinar suspension cells isolated from Ptf1a<sup>ERT</sup> and Ptf1a<sup>ERT</sup>;R1b<sup>fl/fl</sup> animals. Acinar cells in suspension adapted a progenitor-like profile due to alterations in their transcriptional programme.<sup>43</sup> The ChIP data revealed greatly reduced H2AK119ub levels at the promoter sites of *Klf15*, *Cel* or *Cpa2* in Ring1b-depleted cells (figure 3F), which is associated with increased gene expression (figure 3G). Moreover, H3K27me3 levels were also reduced in Ring1b-depleted acinar cells (figure 3F). Altogether, our findings indicate that ADM and the establishment of a progenitor-like expression profile with the concomitant silencing of differentiation genes is strongly diminished in Ring1b-depleted mice.

### Ring1b-mediated epigenetic changes promote Kras<sup>G12D</sup>-driven pancreatic carcinogenesis

To study the impact of Ring1b-catalysed acinar gene repression on pancreatic tumour development, we intercrossed mutant Kras<sup>G12D</sup> (K\*) into our conditional Ring1b knockout (R1b KO) mouse model (Ptf1a<sup>ERT</sup>;K\*;R1b<sup>fl/fl</sup>). In accordance with previous data, activation of oncogenic Kras in adult acinar cells induced only a few precancerous lesions (1-year time point) (online supplementary figure 4A).<sup>5,7</sup> However, after cerulein-induced tissue damage, Ptf1a<sup>ERT</sup>;K\* mice (sacrificed 3 weeks after the last cerulein application) displayed numerous ADM, AFL and low grade PanIN lesions, affecting approximately 70% of pancreatic tissue mass (figure 4A and B). Twenty-four weeks after treatment, five out of six Ptf1a<sup>ERT</sup>;K\* animals developed high grade PanIN lesions and two out of six had PDAC (figure 4A,B). Strikingly, Ring1b-deficient mice, sacrificed after 3 weeks, exhibited only a few ADM and low-grade PanIN lesions and no high-grade lesions or PDAC were detectable after 24 weeks (figure 4A,B). Immunoblot analysis confirmed reduced Ring1b and H2AK119ub levels in cerulein-administered Ptf1a<sup>ERT</sup>;K\*;R1b<sup>fl/fl</sup> in comparison with Ptf1a<sup>ERT</sup>;K\* mice (3 weeks after cerulein) (figure 4C). Successful Cre-recombination activity was visualised by the expression of tdTomato (figure 4D). Furthermore, immunofluorescence staining of amylase and Ck19 confirmed the presence of abundant ADM and PanIN structures in Ptf1a<sup>ERT</sup>;K\* and a lack of these lesions in Ptf1a<sup>ERT</sup>;K\*;R1b<sup>fl/fl</sup> mice (figure 4D). PanINs were quantified by alcian blue staining, demonstrating the increased presence of the precancerous lesions in Ptf1a<sup>ERT</sup>;K\* animals, whereas amylase was substantially higher expressed in Ptf1a<sup>ERT</sup>;K\*;R1b<sup>fl/fl</sup> animals (figure 4E). mRNA expression of acinar differentiation genes and *Klf15* was massively repressed in cerulein-treated Ptf1a<sup>ERT</sup>;K\* animals, whereas gene expression was more abundant in Ptf1a<sup>ERT</sup>;K\*;R1b<sup>fl/fl</sup> mice (figure 4F and online supplementary figure 4B). Expression of *Rbpj*, *Sox9* and *Ck19* was significantly less induced in Ptf1a<sup>ERT</sup>;K\*;R1b<sup>fl/fl</sup> animals

(figure 4G). In conclusion, these results demonstrated that a loss of Ring1b-triggered epigenetic and transcriptional reprogramming, even in the presence of oncogenic Kras, can greatly diminish PDAC development. Thus, acinar gene silencing catalysed by Ring1b is an essential prerequisite to induce oncogenic cell transformation.

### Ablation of Ring1b in pancreatic TCs establishes a less aggressive phenotype

Since Ring1b expression is greatly elevated in PDAC,<sup>31,44</sup> its presence may be beneficial for sustaining TC malignancy. Hence, we knocked out Ring1b in an aggressive pancreatic TC line (KPC-1050), previously isolated from a Ptf1a<sup>Cre/+</sup>;LSL-Kras<sup>G12D/+</sup>;Trp53<sup>lox/+</sup> mouse by using CRISPR/Cas9. R1b KO (three cell clones) cells showed a complete absence of Ring1b and reduced levels of H2AK119ub, whereas global amounts of H3K27me3 remained unchanged (figure 5A). By performing mRNA expression microarrays, we found 575 genes to be upregulated (FC >1.5) and 376 downregulated genes (FC <0.66) in R1b KO cells. GO terms generated from upregulated genes were mostly related to developmental processes, whereas the majority of downregulated genes was mainly connected to chromatin organisation (figure 5B and online supplementary table 7). The GO terms ‘epithelium development’ and ‘morphogenesis of epithelium’, defined by upregulated genes in R1b KO cells, implied a cellular reprogramming towards a more epithelial phenotype (figure 5B). Indeed, we uncovered significantly increased mRNA expression of *Epcam* in R1b KO cells (online supplementary figure 5A). In the ChIP-seq data of our in vitro carcinogenesis model, we detected a broad enrichment of H2AK119ub at the *Epcam* promoter in TC, identifying *Epcam* as a Ring1b target gene (online supplementary figure 5B).

Moreover, we noticed an increased expression of the acinar differentiation genes *Bhlha15* and *Rbpj* as well as of *Klf15* in R1b KO cells (figure 5C), whereby the *Rbpj* and *Klf15* promoter showed a significant loss of H2AK119ub and an appreciable enrichment of H3K4me3 (figure 5D). These results repeatedly confirmed *Klf15* as a putative Ring1b target gene in pancreatic carcinogenesis.

Further functional characterisation demonstrated significantly decreased colony and sphere formation of R1b KO cells in vitro (figure 5E,F). After orthotopic transplantation of control and R1b KO cells in C57BL/6J mice, we observed tumour formation in all control cell-injected animals (nine out of nine), but only in six out of nine R1b KO cell-transplanted mice (figure 5G). Tumour tissue of R1b KO cells was more necrotic and harboured more immune cell infiltration as indicated by the histology score (figure 5G). In addition, we detected circulating epithelial cells in the blood from seven out of nine control mice, while only two out of eight R1b KO cell-transplanted animals showed circulating epithelial cells (figure 5H). Overall, a loss of Ring1b provokes TC reprogramming towards a less malignant phenotype with decreased invasive properties. Consequently, the maintenance of Ring1b-mediated epigenetic silencing of differentiation and epithelial genes promotes the development of an aggressive pancreatic cancer cell type.

### Ring1b as a promising therapeutic target

To target Ring1b-mediated ubiquitination of H2AK119, we took advantage of the previously described Ring1b inhibitor, a small molecular compound called 2-pyridine-3-yl-methylene-indan-1,3-dione (PRT4165).<sup>45</sup> The inhibitor effectively suppressed Ring1b, whereas other E3 ubiquitin ligases, such as RNF8 or

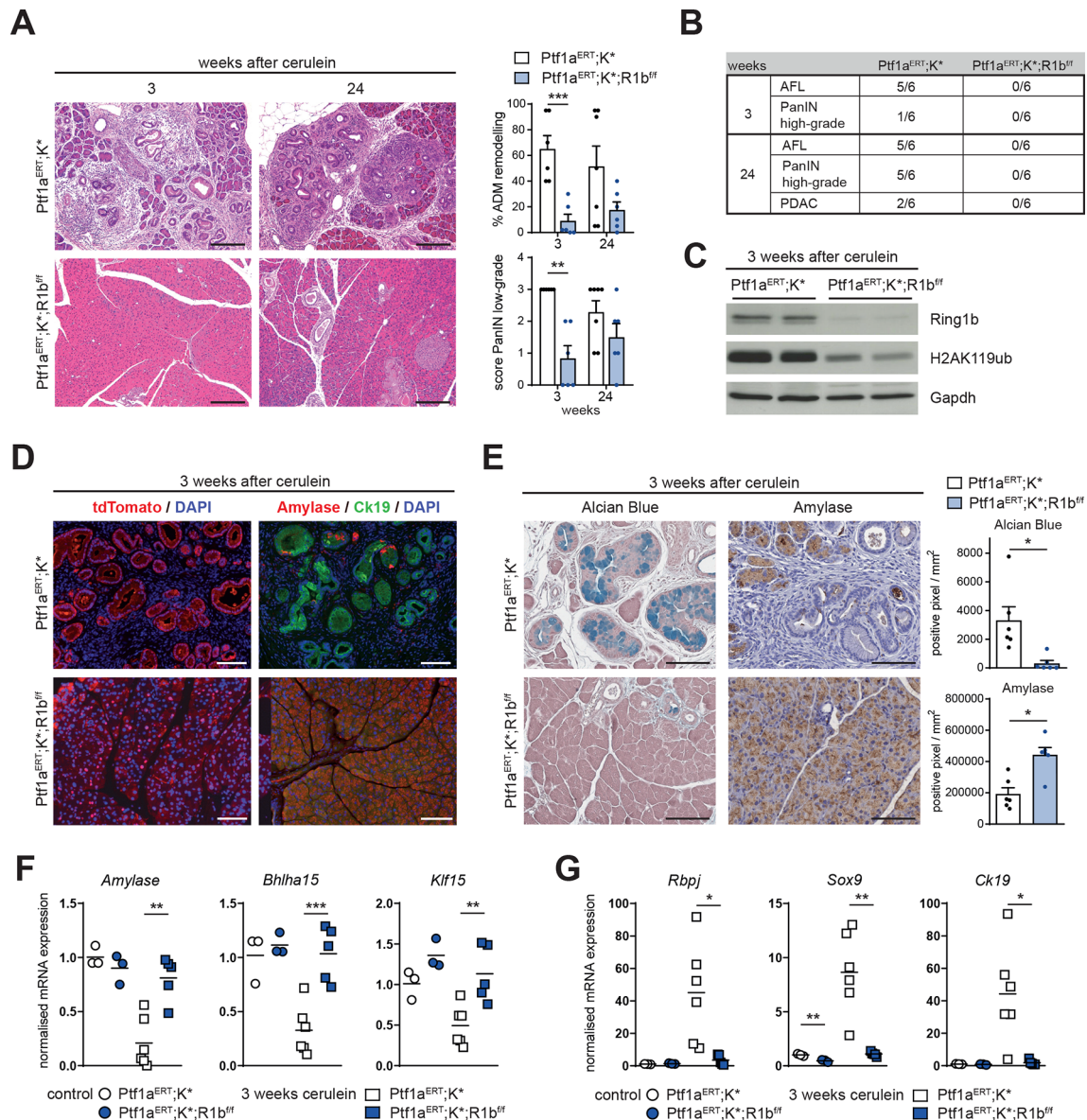
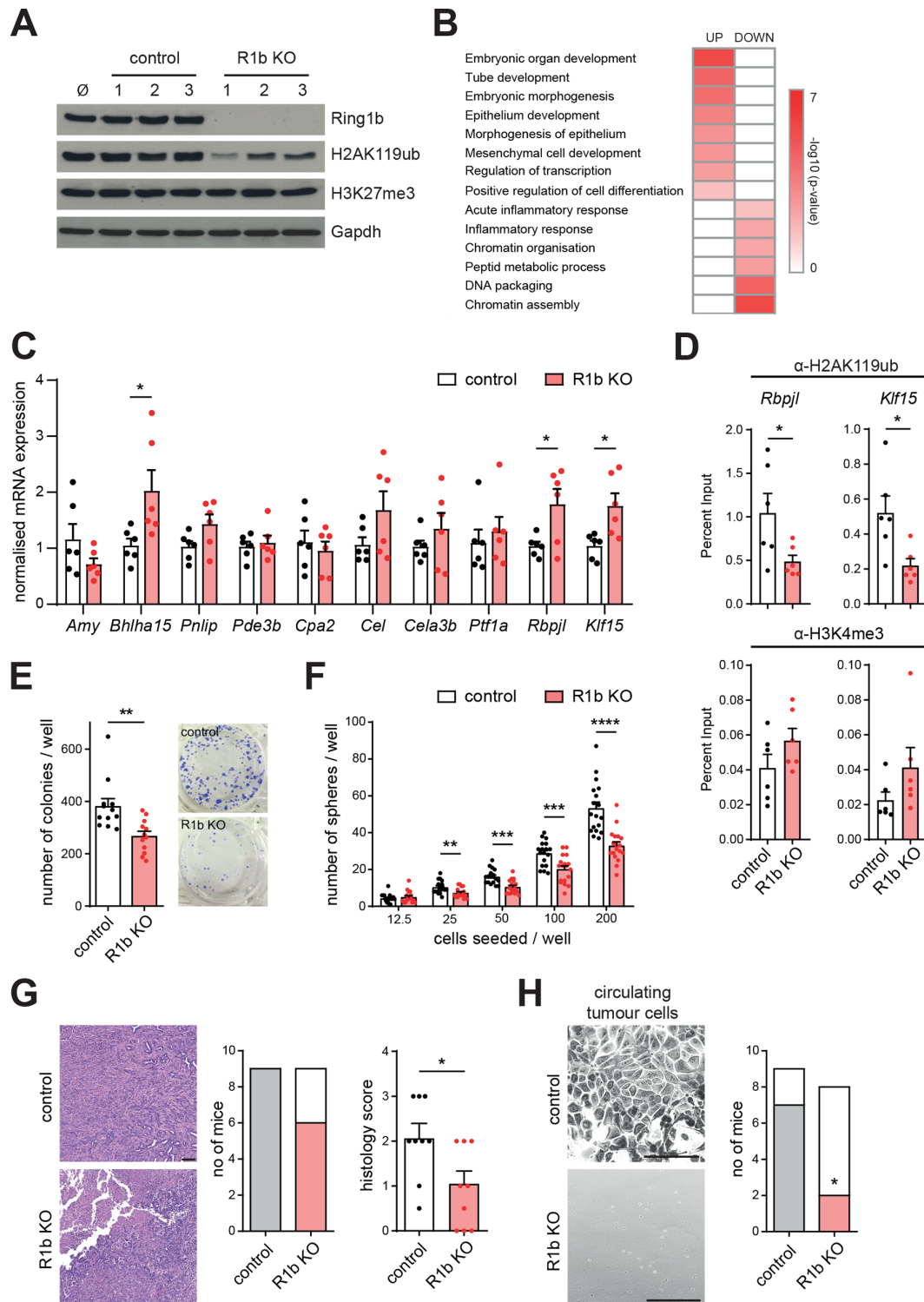


**Figure 4** Ring1b-catalysed epigenetic alterations promote *Kras*<sup>G12D</sup>-driven pancreatic carcinogenesis. (A) Ptf1a<sup>ERT</sup>;K\* and Ptf1a<sup>ERT</sup>;K\*;R1b<sup>ff</sup> mice were treated with tamoxifen (6-week-old) and cerulein (8-week-old). Representative H&E staining depicted 3 and 24 weeks after the last cerulein administration. Scale bars: 200  $\mu$ m. Quantity of ADM remodelling was estimated in per cent to whole slide. Amount of low-grade PanIN was scored and data are represented as mean $\pm$ SEM; p value for PanIN score was calculated by Mann-Whitney test (n=6–7). (B) Presence of AFLs, high-grade PanIN and PDAC was documented. Number of positive mice is shown in relation to the total number. (C) Representative immunoblot analysis of protein lysates from Ptf1a<sup>ERT</sup>;K\* and Ptf1a<sup>ERT</sup>;K\*;R1b<sup>ff</sup> mice (3-week time point) with indicated antibodies. Gapdh served as loading control (n=2). (D) Representative immunofluorescence staining for tdTomato (left panel), amylase and Ck19 (right panel) of pancreatic tissue from Ptf1a<sup>ERT</sup>;K\* and Ptf1a<sup>ERT</sup>;K\*;R1b<sup>ff</sup> mice (3-week time point). Nuclei were stained with 4',6-diamidino-2-phenylindole (DAPI). Scale bars: 100  $\mu$ m. (E) Immunohistochemical analysis of amylase as well as alcian blue staining (3-week time point). Positive pixel were quantified with QuPath and related to the total area. Scale bars: 100  $\mu$ m (n=6). (F) mRNA expression analysis of acinar differentiation genes of control and cerulein-injected (3-week time point) Ptf1a<sup>ERT</sup>;K\* and Ptf1a<sup>ERT</sup>;K\*;R1b<sup>ff</sup> mice (n=3–6). (G) mRNA expression analysis of progenitor genes in the same context as described in figure part F (n=3–6). Unless otherwise stated, all data are represented as mean $\pm$ SEM; p values were calculated by two-tailed, unpaired Student's t-test; \*P<0.05, \*\*p<0.01, \*\*\*p<0.001. ADM, acinar-to-ductal metaplasia; AFL, atypical flat lesion; PanIN, pancreatic intraepithelial neoplasia; PDAC, pancreatic ductal adenocarcinoma.

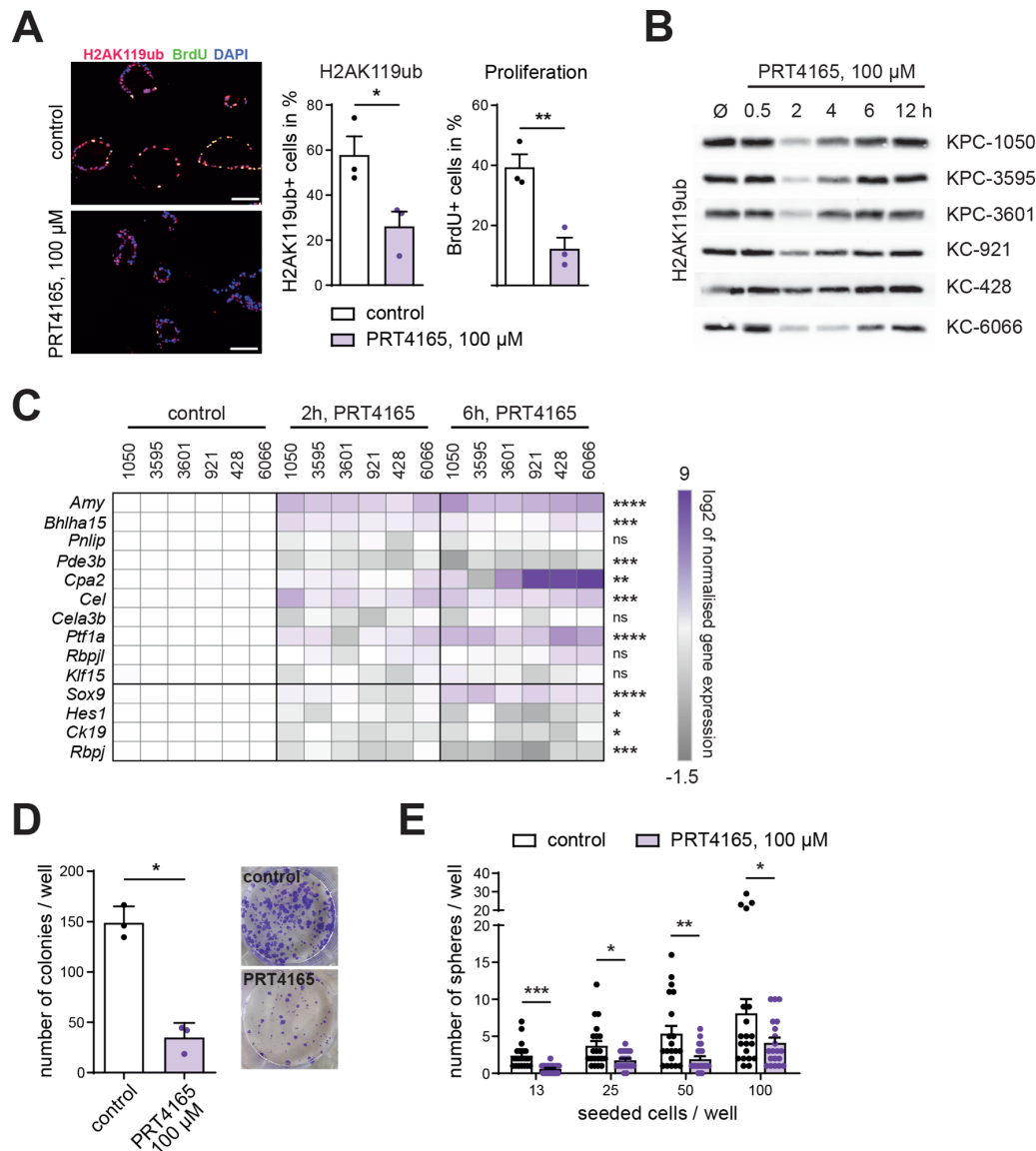
RNF168 were barely affected.<sup>46</sup> First, we tested the impact of PRT4165 on in vitro ADM formation of embedded wildtype acinar cells. Compared with controls, PRT4165 administration resulted in a decreased number of H2AK119ub-positive and proliferating cells as assessed by the BrdU staining (figure 6A). ADM size of treated acinar cell explants was greatly diminished, although the quantity was not affected (online supplementary

figure 6A). PRT4165 treatment of pancreatic TC lines (KPC-1050, KPC-3595, KPC-3601, KC-921, KC-428 and KC-6066) caused decreased levels of H2AK119ub at 2 and 4 hours after inhibitor administration (figure 6B and online supplementary figure 6B). Interestingly, the acinar differentiation genes *Cel*, *Ptf1a* or *Amylase* were significantly upregulated after PRT4165 administration, whereas the expression of the tumour-related genes





**Figure 5** Ablation of Ring1b in pancreatic tumour cells establishes a less aggressive phenotype. (A) Representative immunoblot analysis with the indicated antibodies from protein lysates of untransfected ( $\emptyset$ ), CRISPR/Cas9 control-transfected (control) and CRISPR/Cas9-catalysed Ring1b knockout (R1b KO) murine pancreatic cancer cells (KPC-1050). Gapdh served as loading control. (B) Heatmap of GO terms (biological process), which are significantly enriched or diminished in R1b KO cells. Colour scale represents  $-\log_{10}$  p value. (C) mRNA expression analysis of indicated acinar-specific genes in control and R1b KO cancer cell clones (three clones, n=2). (D) Levels of H2AK119ub and H3K4me3 at the *Rbpjl* and *Klf15* promoter in control and R1b KO cells were evaluated by ChIP analysis. Enrichment was calculated as per cent of input (three clones, n=2). (E) Representative pictures and quantification of colony formation of control and R1b KO cells (three clones, n=4). (F) Quantification of spheroid formation of control and R1b KO cells (three clones, n=6). (G) Representative H&E staining of orthotopic tumours from nine control cell-injected and nine R1b KO tumour cell-injected mice (three mice per clone), graphs show number of mice exhibiting tumour growth and a histology score for tumour evaluation. P value of histology score was calculated by Mann-Whitney test. (H) Representative pictures of blood-isolated circulating epithelial cells from orthotopic tumour mice. Number of mice with positive cultivation of epithelial cells is depicted (n=8–9). Scale bars: 100  $\mu$ m. All data are represented as mean  $\pm$  SEM. Unless otherwise stated, all p values were calculated by two-tailed, unpaired Student's t-test; \*P<0.05, \*\*p<0.01, \*\*\*p<0.001, \*\*\*\*p<0.0001. GO, gene ontology.



**Figure 6** Ring1b as a promising therapeutic target. (A) Representative immunofluorescence staining, detecting H2AK119ub-positive and BrdU-positive cells of control-treated and PRT4165-treated (100  $\mu$ M) wildtype acinar cell explants in a three-dimensional collagen matrix. Cell nuclei were counterstained with DAPI. Five representative pictures were taken and number of H2AK119ub-positive and BrdU-positive cells (proliferation) is represented in relation to the total number of cells. Scale bars: 50  $\mu$ m (n=3). (B) Representative immunoblots detecting H2AK119ub levels after PRT4165 treatment (100  $\mu$ M) at indicated time points in three KPC (1050, 3595 and 3601) and three KC (921, 428 and 6066) cell lines. The corresponding Gapdh loading controls are provided in online supplementary figure 6B. (C) mRNA gene expression of selected genes in KPC (1050, 3595 and 3601) and KC (921, 428 and 6066) tumour cell lines treated with 100  $\mu$ M PRT4165 for 2 and 6 hours was determined by qRT-PCR (n=2). Relative expression levels are visualised within a heatmap. P values were calculated by two-way analysis of variance. (D) Representative pictures and quantification of colony formation of control and 100  $\mu$ M PRT4165-treated KPC-1050 tumour cells (1-day time point) (n=3). (E) Spheroid formation of KPC-1050 tumour cells treated for 24 hours with 100  $\mu$ M PRT4165 (n=20 wells). All data are represented as mean $\pm$ SEM. Unless otherwise stated, p values were calculated by two-tailed, unpaired t-test; \*P<0.05, \*\*p<0.01, \*\*\*p<0.001, \*\*\*\*p<0.0001.

*Rbpj* and *Ck19* was concomitantly reduced (figure 6C). However, *Klf15* expression was persistently down. TC reprogramming of the aggressive cell line KPC-1050 towards a more differentiated phenotype was verified in functional assays showing significantly reduced colony and sphere formation after PRT4165 application (figure 6D,E). In summary, administration of the Ring1b inhibitor PRT4165 decreased ADM formation in vitro and impaired TC aggressiveness, opening new avenues for PDAC treatment.

## DISCUSSION

Epigenetic silencing of tumour suppressor genes, such as *CDKN2A*, was described as a hallmark of cancer contributing

to pancreatic cancer development and progression.<sup>47</sup> Although tissue-specific genes controlling cell homeostasis are downregulated during carcinogenesis, the regulatory mechanisms have been rarely specified. Importantly, the susceptibility of pancreatic acinar cells towards oncogenic transformation highly depends on the cellular reprogramming towards a progenitor-like cell state.<sup>5,7</sup> In the present study, we demonstrated that dynamic epigenetic changes of cell fate regulatory transcription factors and functional acinar genes vigorously transforms acinar cell identity and differentiation promoting acinar cell metaplasia and pancreatic cancer progression. We globally mapped the histone modifications H3K4me3, representing transcriptional activation

and H3K27me3 and H2AK119ub, mediating gene repression, in an in vitro carcinogenesis model to comprehend epigenetic deregulation. Particularly, in comparison with differentiated acinar cells, we identified a significant gain of H3K27me3 and H2AK119ub at the regulatory acinar cell fate genes *Rbpjl*, *Ptf1a*, *Nr5a2* and *Bhlha15* in embryonic acinar and ADM cells with an additional significant loss of H3K4me3 in TCs. Moreover, the transcription factor Klf15 exhibited a similar epigenetic pattern, suggesting a role in regulating acinar cell homeostasis. Notably, in embryonic acinar and ADM cells, the identified acinar differentiation genes were bivalent, reflected by the simultaneous presence of active and repressive histone marks, probably enabling short-term flexibility and acinar cell plasticity. Chromatin bivalency in ADM may be resolved to either re-establish an acinar phenotype or, under oncogenic Kras expression, to transform into TCs. Knockout of *Ptf1a*, *Bhlha15* or *Nr5a2* potentiated ADM and significantly accelerated Kras-dependent PDAC development,<sup>35 37 38</sup> suggesting that the inhibition of acinar genes is critical for pancreatic carcinogenesis. As a novelty, our data revealed the enormous extent of epigenetic deregulation in acinar cell reprogramming and pancreatic cancer progression. In accordance with our previous study, the enrichment of the Ring1b-catalysed histone modification H2AK119ub promotes epigenetic silencing of known and newly identified regulatory acinar cell fate genes.<sup>31</sup>

Consistent with these results, a conditional loss of Ring1b in our mouse model greatly impaired ADM formation, because acinar cells were retained in a differentiated state. Even in the presence of oncogenic Kras, Ring1b depletion significantly diminished vulnerability to oncogenic transformation resulting in massively diminished ADM, PanIN and cancer development. Accordingly, the conditional loss of the PRC1 component Bmi1 in a Kras-driven pancreatic cancer mouse model showed an analogous phenotype with abolished tumour formation.<sup>48</sup> In contrast, a depletion of the PRC2 component Ezh2, catalysing H3K27me3, in embryonic pancreatic cells slightly aggravated early Kras<sup>G12D</sup>-dependent metaplastic tissue transformation but decelerated tumour progression.<sup>49</sup> Overall, the data emphasise a fundamental role of Ring1b-mediated epigenetic silencing of acinar specific genes in initial cellular dedifferentiation and Kras-driven tumour formation.

Moreover, high levels of H2AK119ub in PDAC tissue correlated with a higher tumour grade, larger tumour size as well as lymph node invasion.<sup>50</sup> In our study, loss of Ring1b in established pancreatic cancer cells induced a more epithelial-like and better differentiated phenotype. Accordingly, Ring1b-targeted repression of *E-cadherin* was previously identified.<sup>51</sup> A TC reprogramming was similarly achieved by using the Ring1b inhibitor PRT4165, opening new paths for PDAC therapies.

In conclusion, we delineate Ring1b-mediated epigenetic repression of regulatory cell fate genes as a novel key mechanism triggering acinar cell dedifferentiation and pancreatic cancer development. Thus, epigenetic reprogramming of TCs towards a better differentiated phenotype could represent an effective strategy for cancer therapy.

#### Author affiliations

<sup>1</sup>Department of Medicine II, University Hospital, LMU Munich, Munich, Germany

<sup>2</sup>Department of Molecular and Integrative Physiology, University of Michigan, Ann Arbor, Michigan, USA

<sup>3</sup>Bioinformatic Unit, Biomedical Center, Faculty of Medicine, LMU Munich, Munich, Germany

<sup>4</sup>Quantitative Biology Center, University of Tuebingen, Tuebingen, Germany

<sup>5</sup>Institute of Pathology, Heinrich-Heine University and University Hospital, Dusseldorf, Germany

<sup>6</sup>Department of Surgery, Technical University Munich, Munich, Germany

<sup>7</sup>Institute of Pathology, Technical University Munich, Munich, Germany

<sup>8</sup>Institute of Pathology, Heinrich-Heine-Universität Dusseldorf, Dusseldorf, Germany

<sup>9</sup>Department of Surgery, Martin-Luther University Halle-Wittenberg, Halle (Saale), Germany

**Acknowledgements** The authors would like to thank Nadja Maeritz, Isabell Schäffer and Maria del Socorro Escobar López for their excellent technical support and acknowledge Andreas Dahl at the Center for Molecular and Cellular Bioengineering, Technical University Dresden, Germany and the Department of Clinical Chemistry at the Technical University of Munich, Germany, for sample analyses.

**Funding** The work was supported in part by the Deutsche Forschungsgemeinschaft (DFG) RE 3754/2-1.

**Competing interests** None declared.

**Provenance and peer review** Not commissioned; externally peer reviewed.

#### ORCID iD

Ivonne Regel <http://orcid.org/0000-0002-0206-4441>

#### REFERENCES

- Rahib L, Smith BD, Aizenberg R, *et al.* Projecting cancer incidence and deaths to 2030: the unexpected burden of thyroid, liver, and pancreas cancers in the United States. *Cancer Res* 2014;74:2913–21.
- Siegel RL, Miller KD, Jemal A. Cancer statistics, 2019. *CA Cancer J Clin* 2019;69:7–34.
- Aichler M, Seiler C, Tost M, *et al.* Origin of pancreatic ductal adenocarcinoma from atypical flat lesions: a comparative study in transgenic mice and human tissues. *J Pathol* 2012;226:723–34.
- Morris JP, Cano DA, Sekine S, *et al.* Beta-catenin blocks Kras-dependent reprogramming of acini into pancreatic cancer precursor lesions in mice. *J Clin Invest* 2010;120:508–20.
- Kopp JL, von Figura G, Mayes E, *et al.* Identification of Sox9-dependent acinar-to-ductal reprogramming as the principal mechanism for initiation of pancreatic ductal adenocarcinoma. *Cancer Cell* 2012;22:737–50.
- Storz P. Acinar cell plasticity and development of pancreatic ductal adenocarcinoma. *Nat Rev Gastroenterol Hepatol* 2017;14:296–304.
- Guerra C, Schuhmacher AJ, Cañamero M, *et al.* Chronic pancreatitis is essential for induction of pancreatic ductal adenocarcinoma by K-Ras oncogenes in adult mice. *Cancer Cell* 2007;11:291–302.
- Kong B, Bruns P, Behler NA, *et al.* Dynamic landscape of pancreatic carcinogenesis reveals early molecular networks of malignancy. *Gut* 2018;67:146–56.
- Jensen JN, Cameron E, Garay MV, *et al.* Recapitulation of elements of embryonic development in adult mouse pancreatic regeneration. *Gastroenterology* 2005;128:728–41.
- Rooman I, Real FX. Pancreatic ductal adenocarcinoma and acinar cells: a matter of differentiation and development? *Gut* 2012;61:449–58.
- Hruban RH, Iacobuzio-Donahue C, Wilentz RE, *et al.* Molecular pathology of pancreatic cancer. *Cancer J* 2001;7:251–8.
- Jones S, Zhang X, Parsons DW, *et al.* Core signaling pathways in human pancreatic cancers revealed by global genomic analyses. *Science* 2008;321:1801–6.
- Waddell N, Pajic M, Patch AM, *et al.* Whole genomes redefine the mutational landscape of pancreatic cancer. *Nature* 2015;518:495–501.
- McDonald OG, Li X, Saunders T, *et al.* Epigenomic reprogramming during pancreatic cancer progression links anabolic glucose metabolism to distant metastasis. *Nat Genet* 2017;49:367–76.
- Roe JS, Hwang CI, Somerville TDD, *et al.* Enhancer reprogramming promotes pancreatic cancer metastasis. *Cell* 2017;170:875–.
- Diaferia GR, Balestrieri C, Prosperini E, *et al.* Dissection of transcriptional and cis-regulatory control of differentiation in human pancreatic cancer. *Embo J* 2016;35:595–617.
- Flavahan WA, Gaskell E, Bernstein BE. Epigenetic plasticity and the hallmarks of cancer. *Science* 2017;357:eaal2380.
- Schuettengruber B, Martinez AM, Iovino N, *et al.* Trithorax group proteins: switching genes on and keeping them active. *Nat Rev Mol Cell Biol* 2011;12:799–814.
- Bracken AP, Kleine-Kohlbrecher D, Dietrich N, *et al.* The Polycomb group proteins bind throughout the INK4A-ARF locus and are disassociated in senescent cells. *Genes Dev* 2007;21:525–30.
- Leeb M, Wutz A. Ring1B is crucial for the regulation of developmental control genes and PRC1 proteins but not X inactivation in embryonic cells. *J Cell Biol* 2007;178:219–29.
- Sparmann A, van Lohuizen M. Polycomb silencers control cell fate, development and cancer. *Nat Rev Cancer* 2006;6:846–56.
- Kopinke D, Brailsford M, Pan FC, *et al.* Ongoing notch signaling maintains phenotypic fidelity in the adult exocrine pancreas. *Dev Biol* 2012;362:57–64.
- Jackson EL, Willis N, Mercer K, *et al.* Analysis of lung tumor initiation and progression using conditional expression of oncogenic K-ras. *Genes Dev* 2001;15:3243–8.

- 24 Madisen L, Zwingman TA, Sunkin SM, *et al.* A robust and high-throughput Cre reporting and characterization system for the whole mouse brain. *Nat Neurosci* 2010;13:133–40.
- 25 Calés C, Román-Trufero M, Pavón L, *et al.* Inactivation of the polycomb group protein Ring1B unveils an antiproliferative role in hematopoietic cell expansion and cooperation with tumorigenesis associated with Ink4a deletion. *Mol Cell Biol* 2008;28:1018–28.
- 26 Andricovich J, Perkill S, Kai Y, *et al.* Loss of KDM6A activates super-enhancers to induce gender-specific squamous-like pancreatic cancer and confers sensitivity to BET inhibitors. *Cancer Cell* 2018;33:512–26.
- 27 Collisson EA, Sadanandam A, Olson P, *et al.* Subtypes of pancreatic ductal adenocarcinoma and their differing responses to therapy. *Nat Med* 2011;17:500–3.
- 28 Norberg KJ, Nania S, Li X, *et al.* RCAN1 is a marker of oxidative stress, induced in acute pancreatitis. *Pancreatol* 2018;18:734–41.
- 29 Gong F, Clouaire T, Aguirrebengoa M, *et al.* Histone demethylase KDM5A regulates the ZMYND8-NuRD chromatin remodeler to promote DNA repair. *J Cell Biol* 2017;216:1959–74.
- 30 Warner MH, Roinick KL, Arndt KM. Rtf1 is a multifunctional component of the Paf1 complex that regulates gene expression by directing cotranscriptional histone modification. *Mol Cell Biol* 2007;27:6103–15.
- 31 Benitz S, Regel I, Reinhard T, *et al.* Polycomb repressor complex 1 promotes gene silencing through H2AK119 mono-ubiquitination in acinar-to-ductal metaplasia and pancreatic cancer cells. *Oncotarget* 2016;7:11424–33.
- 32 Pan G, Tian S, Nie J, *et al.* Whole-genome analysis of histone H3 lysine 4 and lysine 27 methylation in human embryonic stem cells. *Cell Stem Cell* 2007;1:299–312.
- 33 Endoh M, Endo TA, Endoh T, *et al.* Histone H2A mono-ubiquitination is a crucial step to mediate PRC1-dependent repression of developmental genes to maintain ES cell identity. *PLoS Genet* 2012;8:e1002774.
- 34 Zhang T, Cooper S, Brockdorff N. The interplay of histone modifications - writers that read. *EMBO Rep* 2015;16:1467–81.
- 35 Krah NM, De La O JP, Swift GH, De La O J SGH, *et al.* The acinar differentiation determinant PTF1A inhibits initiation of pancreatic ductal adenocarcinoma. *Elife* 2015;4.
- 36 Beres TM, Masui T, Swift GH, *et al.* PTF1 is an organ-specific and Notch-independent basic helix-loop-helix complex containing the mammalian Suppressor of Hairless (RBP-J) or its paralogue, RBP-L. *Mol Cell Biol* 2006;26:117–30.
- 37 Shi G, Zhu L, Sun Y, *et al.* Loss of the acinar-restricted transcription factor Mist1 accelerates Kras-induced pancreatic intraepithelial neoplasia. *Gastroenterology* 2009;136:1368–78.
- 38 von Figura G, Morris JP, Wright CV, *et al.* Nr5a2 maintains acinar cell differentiation and constrains oncogenic Kras-mediated pancreatic neoplastic initiation. *Gut* 2014;63:656–64.
- 39 Mori T, Sakae H, Iguchi H, *et al.* Role of Krüppel-like factor 15 (KLF15) in transcriptional regulation of adipogenesis. *J Biol Chem* 2005;280:12867–75.
- 40 Mallipattu SK, Liu R, Zheng F, *et al.* Kruppel-like factor 15 (KLF15) is a key regulator of podocyte differentiation. *J Biol Chem* 2012;287:19122–35.
- 41 Sachs M, Onodera C, Blaschke K, *et al.* Bivalent chromatin marks developmental regulatory genes in the mouse embryonic germline in vivo. *Cell Rep* 2013;3:1777–84.
- 42 Lee S, Hong SW, Min BH, *et al.* Essential role of clusterin in pancreas regeneration. *Dev Dyn* 2011;240:605–15.
- 43 Pinho AV, Rooman I, Reichert M, *et al.* Adult pancreatic acinar cells dedifferentiate to an embryonic progenitor phenotype with concomitant activation of a senescence programme that is present in chronic pancreatitis. *Gut* 2011;60:958–66.
- 44 Martínez-Romero C, Rooman I, Skoudy A, *et al.* The epigenetic regulators Bmi1 and Ring1B are differentially regulated in pancreatitis and pancreatic ductal adenocarcinoma. *J Pathol* 2009;219:205–13.
- 45 Alchanati I, Teicher C, Cohen G, *et al.* The E3 ubiquitin-ligase Bmi1/Ring1A controls the proteasomal degradation of Top2alpha cleavage complex - a potentially new drug target. *PLoS One* 2009;4:e8104.
- 46 Ismail IH, McDonald D, Strickfaden H, *et al.* A small molecule inhibitor of polycomb repressive complex 1 inhibits ubiquitin signaling at DNA double-strand breaks. *J Biol Chem* 2013;288:26944–54.
- 47 Schutte M, Hruban RH, Geradts J, *et al.* Abrogation of the Rb/p16 tumor-suppressive pathway in virtually all pancreatic carcinomas. *Cancer Res* 1997;57:3126–30.
- 48 Bednar F, Schofield HK, Collins MA, *et al.* Bmi1 is required for the initiation of pancreatic cancer through an Ink4a-independent mechanism. *Carcinogenesis* 2015;36:730–8.
- 49 Chen NM, Neesse A, Dyck ML, *et al.* Context-dependent epigenetic regulation of nuclear factor of activated t cells 1 in pancreatic plasticity. *Gastroenterology* 2017;152:1507–20.
- 50 Chen S, Chen J, Zhan Q, *et al.* H2AK119Ub1 and H3K27Me3 in molecular staging for survival prediction of patients with pancreatic ductal adenocarcinoma. *Oncotarget* 2014;5:10421–33.
- 51 Chen J, Xu H, Zou X, *et al.* Snail recruits Ring1B to mediate transcriptional repression and cell migration in pancreatic cancer cells. *Cancer Res* 2014;74:4353–63.